Bioorg. Med. Chem. Lett. 50 (2021) 128328

Contents lists available at ScienceDirect

Bioorganic & Medicinal Chemistry Letters

journal homepage: www.elsevier.com/locate/bmcl

Installation of high-affinity Siglec-1 ligand on tumor surface for macrophage-engaged tumor suppression

Enkang Zhang [a], Shixiong Wen [b], Jialiang Quan [a], Jiahuai Han [b], Hongzhi Cao [c], Shoufa Han [a,*]

[a] Department of Chemical Biology, College of Chemistry and Chemical Engineering, The Key Laboratory for Chemical Biology of Fujian Province, State Key Laboratory for Physical Chemistry of Solid Surfaces and The MOE Key Laboratory of Spectrochemical Analysis & Instrumentation, Xiamen University, Xiamen, China
[b] State Key Laboratory of Cellular Stress Biology, Innovation Center for Cell Signaling Network, School of Life Sciences, Xiamen University, Xiamen, China
[c] Key Laboratory of Marine Drugs of Ministry of Education, and Laboratory for Marine Drugs and Bioproducts of Qingdao National Laboratory for Marine Science and Technology, School of Medicine and Pharmaceutics, Ocean University of China, Qingdao, China

ARTICLE INFO

Keywords:
Sialic acid-binding immunoglobulin-like lectins (Siglecs)
Siglec ligands
Tumor suppression

ABSTRACT

Siglecs that binds cell surface sialoglycans are a family of immunomodulatory receptors, of which, Siglec-7 expressed on natural killer (NK) cells promotes tumor immunoevation while the role of Siglec-1 expressed on macrophages on tumor development remains largely unexplored. Herein, we selectively introduced high affinity sialoside ligands of Siglec-1 and Siglec-7 to tumor cell surface via in vivo Strain-promoted Azide-Alkyne cyclization of ^{TCC}Siaα2,3-Lactose or ^{FITC}Siaα2,6-Lactose with 9-azido sialic acid (^{Az}Sia) metabolically installed on tumor cell surface. We found that ^{TCC}Siaα2,3-Lactose conjugated on tumor surface moderately inhibited tumor growth while ^{FITC}Siaα2,6-Lactose promote tumor growth. These results suggest high-affinity ligand of Siglec-1 dispalyed on tumors surface provide a new perspective for tumor immunotherapy.

Siglecs, a family of sialic acid-binding immunoglobulin-like lectins, have been defined as immune cell glyco-checkpoints in disease.[1–8] Most of the Siglecs have a immunoreceptor tyrosine-based inhibitory motif (ITIM) served as negative regulatory receptor.[1,9] For example, Siglec-7 on natural killer (NK) cells is a negative regulator of NK-mediated cell killing of tumor cells that express Siglec-7 ligand.[5,6,10–12] However, Siglec-1, expressed on macrophages which lacks ITIM.[9] To date, how the binding of Siglec-1 to tumor surface glycans affects tumor development remains largely unexplored. As ^{TCC}Siaα2,3-Lactose and ^{FITC}Siaα2,6-Lactose are reported as selective high-affinity ligands of Siglec-1 and Siglec-7, respectively,[13,14] we sought to introduce high-affinity Siglec-1 ligand on tumor cell surface by metabolic glycan labeling (MGL), aiming to examine its performance to recruit macrophages and to suppress tumor growth.

MGL emploits substrate promiscuity of Sia biosynthetic pathway to modify cell syrface glycans with abiotic Sia bearing unique chemical handles such as azide.[15–19] The azide could be bioorthogonally labeled for diverse purposes such as cell surface glycan imaging and tumour treatment.[15–22] We first utilized MGL to modify tumor cell surface on mice models with ^{Az}Sia with the aid of ligand-targeted liposomes (^{Az}Sia@LP-Biotin), and then intravenously inject aza-dibenzocyclooctyne (DBCO)-conjugated high-affinity ligands of Siglec-1 (^{TCC}Siaα2,3-Lac-DBCO) or Siglec-7 (^{FITC}Siaα2,3-Lac-DBCO) to covalently label ^{Az}Sia expressed on tumor surface via Strain-promoted Azide-Alkyne cyclization (SPAAC)[23–26] (Fig. 1). We observed suppression of tumor growth with high-affinity ligand of Siglec-1 while Siglec-7 high-affinity ligand promote tumor growth, suggesting that Siglec-1 that lacks IMIT motif could be potentially exployed for tumor immuotherapy.

To incorporate Siglec-1 ligand on tumor cell suface, we opted biotin-decorated liposomes that encapsulate ^{Az}Sia (^{Az}Sia@LP-Biotin) to metabolically install ^{Az}Sia on biotin recetor-expressing tumor surface over healthy tissues.[27] We prepeared ^{Az}Sia@LP-Biotin (Fig. S1) according to our previous work,[27] and then examined its capacity to metabolically label B16-F10 cells that express high levels of biotin-receptor,[28,29] and exhibit sialic acid-correlated high metastatic potential.[30–31] The cells were incubated with ^{Az}Sia@LP-Biotin for varied periods of time, and then treated with ^{FITC}Siaα2,6-Lac-DBCO via SPAAC. Confocal fluorescence microscopy analysis showed bright green-fluorescense intensity on cell surface as a function of incubation time whereas ^{Az}Sia-free liposomes casued no obvious fluorescence on cell surface, suggesting metabolic labeling of cell-surface glycans in B16-F10 cells (Fig. 2A). We next explored the retention time of ^{FITC}Siaα2,6-Lactose anchored on cell-surface by culturing pre-labeled cells in fresh medium for 24 h. Albeit decreased, sigificant levels of green fluorescense was identified on the

* Corresponding author.
E-mail address: shoufa@xmu.edu.cn (S. Han).

https://doi.org/10.1016/j.bmcl.2021.128328
Received 6 June 2021; Received in revised form 8 August 2021; Accepted 11 August 2021
Available online 20 August 2021

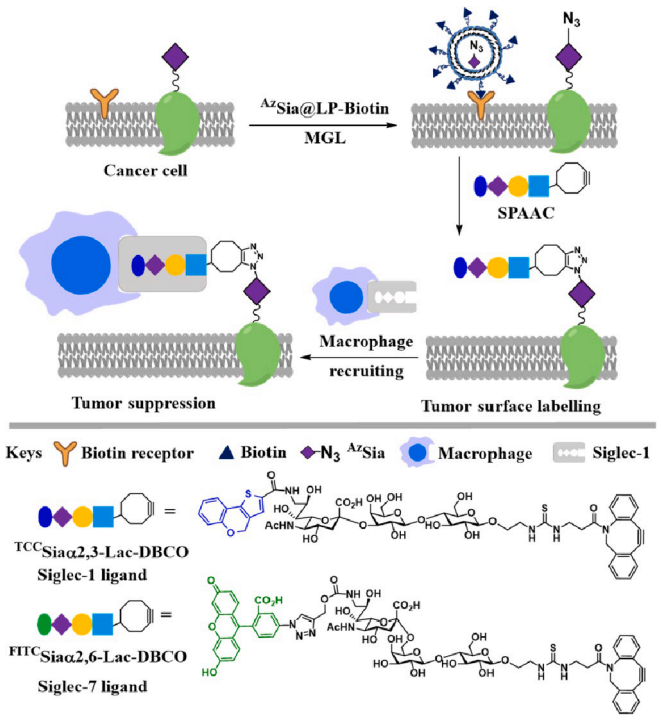

Fig. 1. Schematic for tumor suppression via installation of high-affinity Siglec-1 ligand on tumor surface. ^{Az}Sia@LP-Biotin recognized by the cell-surface receptors expressed on the tumors induces the internalization of the liposomal ^{Az}Sia into the cancer cells. The ^{Az}Sia is utilized by biosynthetic enzymes and incorporated selectively into tumor-associated glycans, and then ^{TCC}Siaα2,3-Lac-DBCO is covalently labeled on the cell membrane by SPAAC in vivo inducing tumor suppression.

cell surface. The 24-h retention time indicated the potential of ^{FITC}Siaα2,6-Lactose ligand conjugated on tumor cell surface to recruit immune cells (Fig. 2B).

We speculated that Siglec$^+$ immune cells could be better recruited to tumor cells by high affinity Siglec ligands installed on tumor cell surface. To test this, we modified ^{Az}Sia$^+$ B16F10 cells with an affinity ligand of Siglec-1 (^{TCC}Siaα2,3-Lac-DBCO) or Siglec-7 (^{FITC}Siaα2,6-Lac-DBCO), and then co-cultured these modified cells (referred to as ^{TCC}Siaα2,3-Lac$^+$ and ^{FITC}Siaα2,6-Lac$^+$) with Siglec-7$^+$ NK92 cells or Siglec-1$^+$ bone marrow derived macrophages (BMDM), repectively. As shown in Fig. 3A, NK92 cells caused aggregation of ^{FITC}Siaα2,6-Lac$^+$ B16-F10 tumor cells as compared to unmodified tumor cells. This confirmed upregulated tumor-immune cell interactions mediated by high affinity Siglec-7 ligand (^{FITC}Siaα2,6-Lactose) incorporated on tumor surfaces. In contrast, cell death was induced by high affinity Siglec-1 ligand installed on tumor surfaces (^{TCC}Siaα2,3-Lac$^+$ cells) in the presence of Siglec-1$^+$ macrophages, as evidenced altered cell shape and genesis of cell debris (Fig. 3B).

We then performed real time course study to image interplay of immune cells with Siglec-ligand$^+$ tumor cells by confocal microscopy. We identified physical contact of macrophages with ^{TCC}Siaα2,3-Lac$^+$ tumor cells over unmodified tumor cells (Fig. 3C). Similar pattern was recapitulated in the interaction of NK cells with ^{FITC}Siaα2,6-Lac$^+$ tumor cells using ligand-free tumor cells as control (Fig. 3C). In addition, we also tested the interplay of Siglec$^+$ immune cells with mismatched ligands incorporated on tumor cell surface. ^{FITC}Siaα2,6-Lac$^+$ B16-F10 cells exhibited no obvious physical contact with Siglec-1$^+$ BMDM, and this also ocurred between and ^{TCC}Siaα2,3-Lac$^+$-B16-F10 cells and Siglec-7$^+$ NK92 cells (Fig. S2). Taken together, these data confirmed tumor-imune cell interaction promoted by Siglecs and their cognate affinity ligands displayed on tumor cell surface.

Next, we explored the influence of Siglec ligands conjugated on

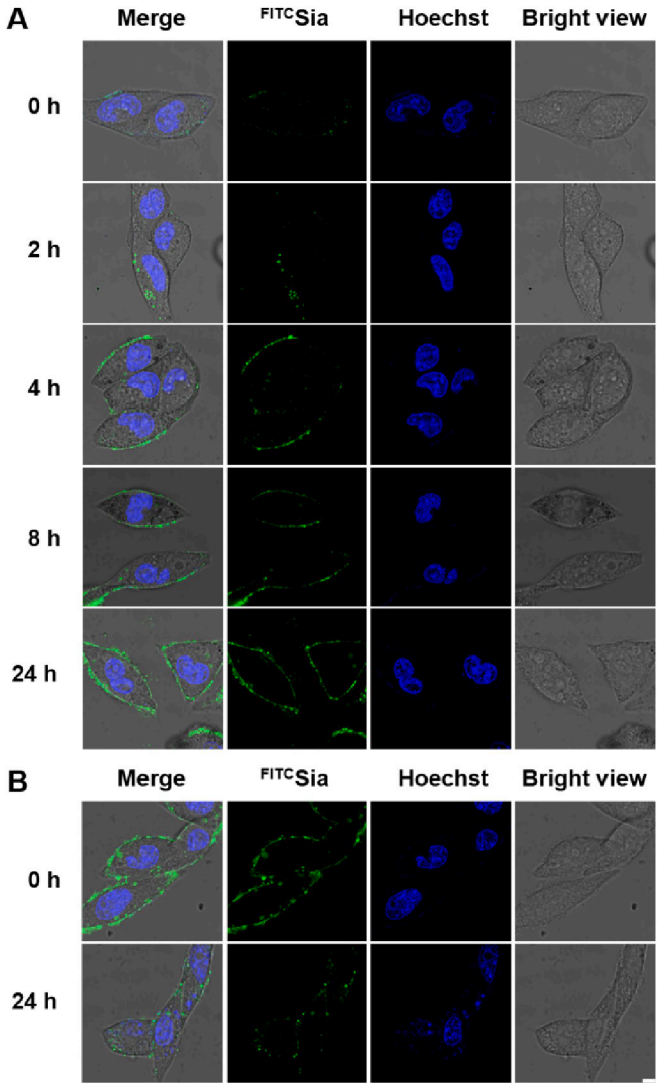

Fig. 2. Covalent labeling of tumor cell surface with high affinity Siglec-7 ligand. (A) B16-F10 cells were incubated with ^{Az}Sia@LP-Biotin for 0–24 h, and then treated with ^{FITC}Siaα2,6-Lac-DBCO (100 μM) before confocal fluorescence microscopic analysis. (B) ^{FITC}Siaα2,6-Lactose-labelled B16-F10 cells were cultured in fresh DMEM for 24 h, and then imaged by confocal fluorescence microscopy. Scale bars, 5 μm.

tumor cell surface on tumor growth in vivo. ^{TCC}Siaα2,3-Lac$^+$, ^{FITC}Siaα2,6-Lac$^+$, or ^{Az}Sia$^+$ B16-F10 cells were subcutaneously inoculated into the C57BL/6 mice, respectively. After 7 day-inoculation, the tumor of ^{TCC}Siaα2,3-Lac$^+$ cells exhibited 50% volume reduction compared to that of ^{Az}Sia$^+$ cells (Fig. 4). This retardation was further confirmed by time course study on tumor sizes after innoculation. For instance, the volume of tumor derived form ^{TCC}Siaα2,3-Lac$^+$ cells remained about 30% smaller than that from the ^{Az}Sia$^+$ cells (Fig. 4). Given the role of Siglec-1 on promoting macrophagic endocytosis and that fact that Siglec-1 lacks intracellular cell signaling activity, this tumor retardation is likely due to endocytosis of tumor cells promoted by Siglec-1 and ^{TCC}Siaα2,3-Lac ligand incorporated on tumor cell surface.

In contrast to tumor retardation on ^{TCC}Siaα2,3-Lac$^+$ cells, the volume of ^{FITC}Siaα2,6-Lac$^+$ tumor increase about 30% over ^{Az}Sia$^+$ tumor (Fig. 4). This is consistent with documented effects of Siglec-7 on NK cells that promote tumor immunosuppression dues to its binding to Sia on tumor surface. We anticipated that the promoted tumor growth by ^{FITC}Siaα2,6-Lactose, a known high affinity ligand of Siglec-7, originated

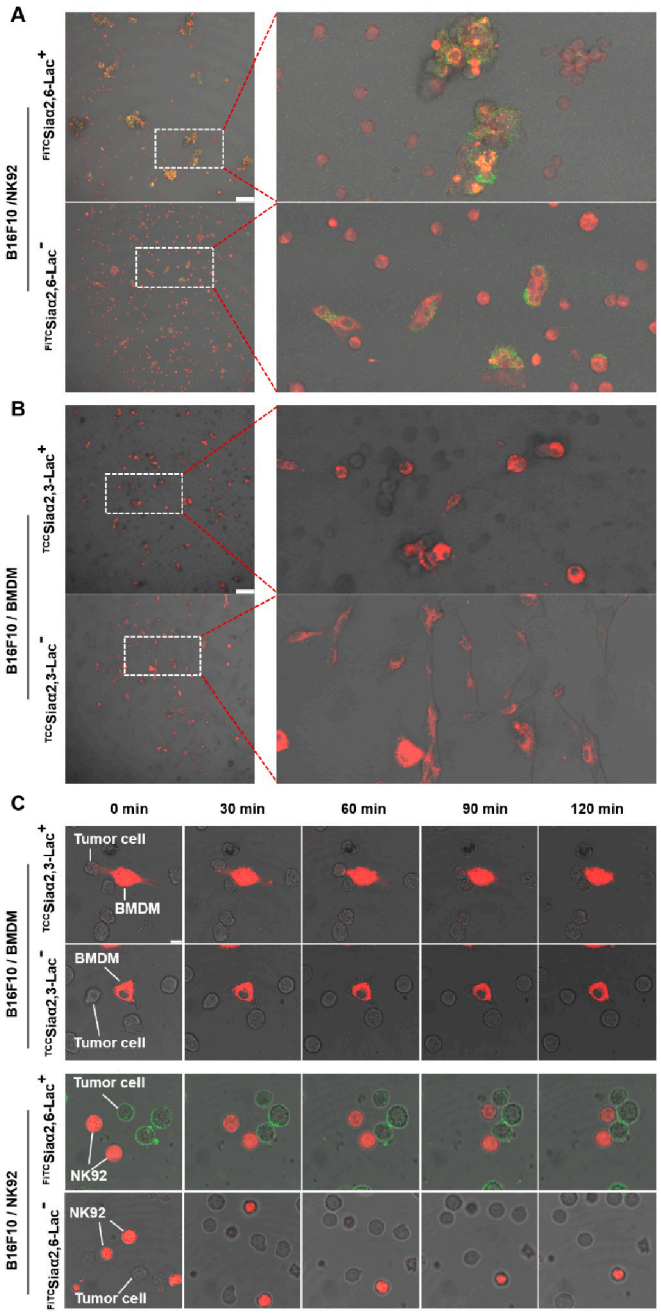

Fig. 3. Tumor-immune cell binding elicited by Siglecs and conjugated high affinity Siglec ligands installed on tumor cell surface. (A) Aggregation of ^{FITC}Siaα2,6-Lac^{+} B16-F10 cells induced by NK cells. B16-F10 cells were labeled with ^{FITC}Siaα2,6-Lac-DBCO while NK92 cells were preststained with red fluorescence using a reported procedure[32]. Scale bars, 25 μm. (B) Cell death of ^{TCC}Siaα2,3-Lac^{+} B16F10 cells by BMDM cells. B16-F10 cells were labeled with ^{TCC}Siaα2,3-Lac-DBCO while BMDM cells were preststained with red fluorescence[32]. Scale bars, 25 μm. (C) Real time imaging of the interaction of immune cells with B16F10 modified with Siglec ligands installed on cell surface. ^{TCC}Siaα2,3-Lac^{+} or ^{TCC}Siaα2,3-Lac^{-} B16-F10 cells were co-cultured with red fluorescence labelled BMDM cells[32], and photos of the cells were taken every 10 mins for 2 h. ^{FITC}Siaα2,6-Lac^{+} or ^{FITC}Siaα2,6-Lac^{-} B16-F10 cells were co-cultured with red fluorescence labelled NK92 cells[32], and photos of the cells were taken every 10 mins for 2 h. Scale bars, 10 μm.

from its binding to Siglec-7 and enhanced tumor immunosuppression thereafter. Taken together, these results demonstrate the potential of Siglec-1 to trigger macrophage-engaged antitumor effects.

With the demonstrated effects of ^{TCC}Siaα2,3-Lactose pre-anchored on

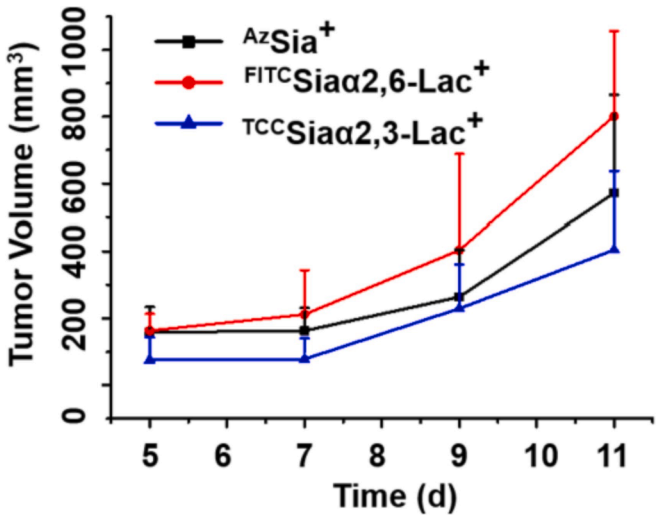

Fig. 4. Differential in vivo immunological responses triggered by high affinity ligands of Siglec-1 and Siglec-7 incorporated tumor cell surface in mice. ^{TCC}Siaα2,3-Lac^{+}, ^{FITC}Siaα2,6-Lac^{+}, and ^{Az}Sia^{+} B16-F10 cells were subcutaneously inoculated into mice which were maintained for 0–11 days. The tumor volumes were measured at 5th, 7th, 9th, and 11th day post inoculation, 3 mice in each group.

tumor cells to inhibit tumor formation, we were keen to determine the antitumor efficacy of in vivo installation of Siglec-1 ligand on tumor cell surface, a condition of clinical relevance. C57BL/6 mice inoculated with B16-F10 cells, kept for 3 days, and intravenously injected with ^{Az}Sia@LP-Biotin via tail-vein. The mice were then injected with ^{TCC}Siaα2,3-Lac-DBCO, using ^{FITC}Siaα2,6-Lac-DBCO and phosphate buffered saline (PBS) as the controls. The mice were kept for 0–14 days and the tumor volume and body weight were regularly monitored (Fig. 5**A-B**). At 14th day, these mice sacrificed, and tumors were dissected. Relative to tumors from mice treated with PBS, administration of ^{TCC}Siaα2,3-Lac-DBCO resulted in 40–50% reduction in tumor volume whereas ^{FITC}Siaα2,6-Lac-DBCO leaded to 110% increase in tumor volume (Fig. 5C), similar results were found in tumor weight statistics (Fig. 5D). In parallel, no obvious effects on body weight were caused by PBS or both glycan ligands (Fig. 5B). The observed inhibitory effects showed the utility of ^{TCC}Siaα2,3-Lactose displayed on tumor surface for systemic tumor suppression, and the applicability of Siglec-1 to boost macrophage-mediated tumor imunotherapy.

In summary, we described the use of Siglec-1 ligand (^{TCC}Siaα2,3-Lactose) incorporated on tumor cell surface via metabolic glycan labeling to elicit macropahge-mediated antitumor effects. In vitro analysis showed that ^{TCC}Siaα2,3-Lactose^{+} cells effectively recriut macrophages and induced tumor cell death. In contrast, albeit recruiting NK cells, Siglec-7 ligand (^{FITC}Siaα2,6-Lactose) did not caused cell death, which is consistent with inmmunoinhibitory roles of Siglec-7 upon its binding to tumor cell surface Sia. Immortantly and consistently, obvious tumor retardation was observed by ^{TCC}Siaα2,3-Lactose that is in vivo conjugated to ^{Az}Sia^{+} tumor cells. Differernt to Siglec-7 on NK cells that could dampen NK cytotoxicty upon its binding to tumor surface Sia, Siglec-1 could promote tumor cell uptake by macropahges and lack the capability to dampen immunoactivity. These results showed the utility of Siglec-1 to boost macrophage-mediated tumor imunotherapy and applicability of metabolically labeled high affinity ligand of Siglec-1 to trigger antitumor effects.

Declaration of Competing Interest

The authors declare that they have no known competing financial interests or personal relationships that could have appeared to influence the work reported in this paper.

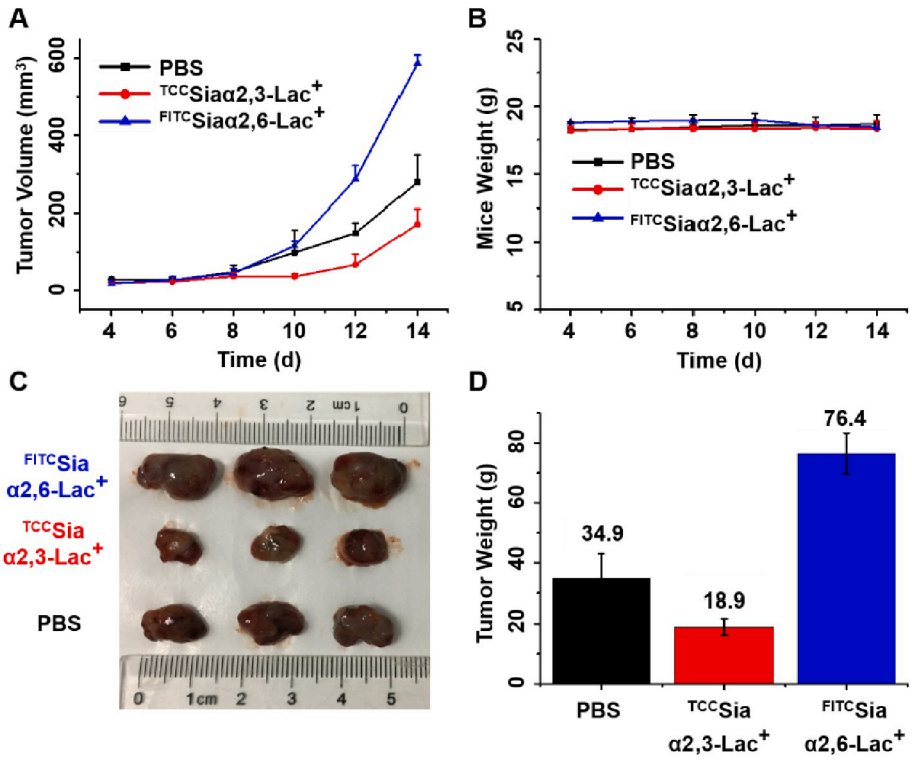

Fig. 5. Tumor suppression via in vivo incorporation of high affinity ligand of Siglec-1 on tumor surface. C57BL/6 mice were inoculated with B16-F10 cells were injected with ^{Az}Sia@LP-Biotin (50 mg/kg, ^{Az}Sia) via tail-vein for 4 h. The mice were further injected with ^{TCC}Siaα2,3-Lac-DBCO, ^{FITC}Siaα2,6-Lac-DBCO or PBS at indicated days post tumor cell inoculation. Tumor volumes and body weights of the mice were monitored over time. (A) Tumor volume measured over time. (B) Body weight of mice measued over time. (C) Tumors were excised and photographed on the 14th day. (D) Statistical image of tumor weight. The assays were performed in quintuplicate, using 5 mice each time.

Acknowledgments

This work was supported by grants from NSF China (91854106, 21775130). Prof. J. Han was supported by NSFC (81788101).

Appendix A. Supplementary data

Supplementary data to this article can be found online at https://doi.org/10.1016/j.bmcl.2021.128328.

References

1 Duan S, Paulson JC. Siglecs as immune cell checkpoints in disease. *Annu Rev Immunol*. 2020;38:365–395.
2 van de Wall S, Santegoets KCM, van Houtum EJH, Büll C, Adema GJ. Sialoglycans and siglecs can shape the tumor immune microenvironment. *Trends Immunol*. 2020; 41:274–285.
3 Barkal AA, Brewer RE, Markovic M, et al. CD24 signalling through macrophage Siglec-10 is a target for cancer immunotherapy. *Nature*. 2019;572:392–396.
4 Wang J, Sun J, Liu LN, et al. Siglec-15 as an immune suppressor and potential target for normalization cancer immunotherapy. *Nat Med*. 2019;25:656–666.
5 Jandus C, Boligan KF, Chijioke O, et al. Interactions between Siglec-7/9 receptors and ligands influence NK cell-dependent tumor immunosurveillance. *J Clin Investig*. 2014;124:1810–1820.
6 Hudak JE, Canham SM, Bertozzi CR. Glycocalyx engineering reveals a Siglec-based mechanism for NK cell immunoevasion. *Nat Chem Biol*. 2014;10:69–75.
7 Macauley MS, Crocker PR, Paulson JC. Siglec-mediated regulation of immune cell function in disease. *Nat Rev Immunol*. 2014;14:653–666.
8 RodrÍguez E, Schetters STT, van Kooyk Y. The tumour glyco-code as a novel immune checkpoint for immunotherapy. *Nat Rev Immunol*. 2018;18:204–211.
9 Angata T, Nycholat CM, Macauley MS. Therapeutic targeting of siglecs using antibody- and glycan-based approaches. *Trends Pharmacol*. 2015;36:645–660.
10 Ikehara Y, Ikehara SK, Paulson JC. Negative regulation of T cell receptor signaling by Siglec-7 (p70/AIRM) and Siglec-9. *J Biol Chem*. 2004;279:43117–43125.
11 Kawasaki Y, Ito A, Withers DA, et al. Ganglioside DSGb5, preferred ligand for Siglec-7, inhibits NK cell cytotoxicity against renal cell carcinoma cells. *Glycobiology*. 2010; 20:1373–1379.
12 Tao L, Wang S, Yang L, Jiang L, Li J, Wang X. Reduced Siglec-7 expression on NK cells predicts NK cell dysfunction in primary hepatocellular carcinoma. *Clin Exp Immunol*. 2020;201:161–170.
13 Edgar LJ, Kawasaki N, Nycholat CM, Paulson JC. Targeted delivery of antigen to activated CD169(+) macrophages induces bias for expansion of CD8(+) T Cells. *Cell Chem Biol*. 2019;26:131–136.
14 Rillahan CD, Schwartz E, Rademacher C, et al. On-chip synthesis and screening of a sialoside library yields a high affinity ligand for Siglec-7. *ACS Chem Biol*. 2013;8: 1417–1422.
15 Saxon E, Bertozzi CR. Cell surface engineering by a modified Staudinger reaction. *Science (New York NY)*. 2000;287:2007–2010.
16 Prescher JA, Dube DH, Bertozzi CR. Chemical remodelling of cell surfaces in living animals. *Nature*. 2004;430:873–877.
17 Haga Y, Ishii K, Hibino K, et al. Visualizing specific protein glycoforms by transmembrane fluorescence resonance energy transfer. *Nat Commun*. 2012;3:907.
18 Griffin ME, Hsieh-Wilson LC. Glycan engineering for cell and developmental biology. *Cell Chem Biol*. 2016;23:108–121.
19 Witte C, Martos V, Rose HM, et al. Live-cell MRI with xenon hyper-CEST biosensors targeted to metabolically labeled cell-surface glycans. *Angew Chem Int Ed*. 2015;54: 2806–2810.
20 Laughlin ST, Bertozzi CR. Metabolic labeling of glycans with azido sugars and subsequent glycan-profiling and visualization via Staudinger ligation. *Nat Protoc*. 2007;2:2930–2944.
21 Laughlin ST, Agard NJ, Baskin JM, et al. Metabolic labeling of glycans with azido sugars for visualization and glycoproteomics. *Meth Enzymol*. 2006;415:230–250.
22 Chang PV, Prescher JA, Sletten EM, et al. Copper-free click chemistry in living animals. *Proc Natl Acad Sci USA*. 2010;107:1821–1826.
23 Agard NJ, Prescher JA, Bertozzi CR. A strain-promoted [3 + 2] azide-alkyne cycloaddition for covalent modification of biomolecules in living systems. *J Am Chem Soc*. 2004;126:15046–15047.
24 Debets MF, van Berkel SS, Schoffelen S, Rutjes FP, van Hest JC, van Delft FL. Aza-dibenzocyclooctynes for fast and efficient enzyme PEGylation via copper-free (3+2) cycloaddition. *Chem Commun (Camb)*. 2010;46:97–99.
25 Xue Z, Zhang E, Liu J, Han J, Han S. Bioorthogonal conjugation directed by a sugar-sorting pathway for continual tracking of stressed organelles. *Angew Chem Int Ed*. 2018;57:10096–10101.
26 Zhang E, Shi Y, Han J, Han S. Organelle-directed metabolic glycan labeling and optical tracking of dysfunctional lysosomes thereof. *Anal Chem*. 2020;92: 15059–15068.
27 Zheng N, Wang S, Su X, Han S. Liposome-aided metabolic engineering of tumor surface immunogenicity. *Bioorg Med Chem Lett*. 2018;28:2550–2554.
28 Bhuniya S, Maiti S, Kim EJ, et al. An activatable theranostic for targeted cancer therapy and imaging. *Angew Chem Int Ed*. 2014;53:4469–4474.
29 Jiang J, Zhao Z, Hai Z, Wang H, Liang G. Intracellular proteolytic disassembly of self-quenched near-infrared nanoparticles turning fluorescence on for tumor-targeted imaging. *Anal Chem*. 2017;89:9625–9628.
30 Yogeeswaran G, Salk PL. Metastatic potential is positively correlated with cell surface sialylation of cultured murine tumor cell lines. *Science (New York, NY)*. 1981; 212:1514–1516.
31 Matsumoto A, Cabral H, Sato N, Kataoka K, Miyahara Y. Assessment of tumor metastasis by the direct determination of cell-membrane sialic acid expression. *Angew Chem Int Ed*. 2010;49:5494–5497.
32 Shi Y, Zhu R, Xue Z, Han J, Han S. An in cellulo-activated multicolor cell labeling approach used to image dying cell clearance. *Analyst*. 2019;144:4687–4693.